Molecular Plant Pathology

MOLECULAR PLANT PATHOLOGY (2018) **19**(11), 2502–2515 DOI: 10.1111/mpp.12722

Technical advance

Transformation by growth onto agro-infiltrated tissues (TGAT), a simple and efficient alternative for transient transformation of the cucurbit powdery mildew pathogen *Podosphaera xanthii*

JESÚS MARTÍNEZ-CRUZ[1,2], DIEGO ROMERO[1,2], ANTONIO DE VICENTE[1,2] AND ALEJANDRO PÉREZ-GARCÍA[1,2*]

[1] *Departamento de Microbiología, Facultad de Ciencias, Universidad de Málaga, Málaga, 29071, Spain*

[2] *Instituto de Hortofruticultura Subtropical y Mediterránea 'La Mayora', Universidad de Málaga, Consejo Superior de Investigaciones Científicas (IHSM-UMA-CSIC), Málaga, 29071, Spain*

SUMMARY

A major limitation of molecular studies in powdery mildew fungi (Erysiphales) is their genetic intractability. This is because they are obligate biotrophs. In these parasites, biotrophy is determined by the presence of haustoria, which are specialized structures of parasitism that play an essential role in the acquisition of nutrients and the deliverance of effectors. *Podosphaera xanthii* is the main causal agent of cucurbit powdery mildew and a major limitation for crop productivity. In a previous study using *P. xanthii* conidia, we showed, for the first time, the transformation of powdery mildew fungi by *Agrobacterium tumefaciens*. In this work, we hypothesized that the haustorium could also act as a natural route for the acquisition of DNA. To test our hypothesis, melon cotyledons were agro-infiltrated with *A. tumefaciens* that contained diverse transfer DNA (T-DNA) constructs harbouring different marker genes under the control of fungal promoters and, after elimination of the bacterium, the cotyledons were subsequently inoculated with *P. xanthii* conidia. Our results conclusively demonstrated the transfer of different T-DNAs from *A. tumefaciens* to *P. xanthii*, including two fungicide resistance markers (*hph* and *tub2*), a reporter gene (*gfp*) and a translational fusion (*cfp-PxEC2*). These results were further supported by the co-localization of translational fluorescent fusions of *A. tumefaciens* VirD2 and *P. xanthii* Rab5 proteins into small vesicles of haustorial and hyphal cells, suggesting endocytosis as the mechanism for T-DNA uptake, presumably by the haustorium. From our perspective, transformation by growth onto agro-infiltrated tissues (TGAT) is the easiest and most reliable method for the transient transformation of powdery mildew fungi.

Keywords: *Agrobacterium tumefaciens*, endocytosis, genetic transformation, haustorium, melon, *Podosphaera xanthii*, powdery mildews.

**Correspondence:* Email: aperez@uma.es

In loving memory of our dear colleague and friend Juan Antonio Torés.

INTRODUCTION

The haustorium-forming fungal pathogens, powdery mildew and rust fungi, represent the largest groups of plant pathogens which, together, cause diseases in thousands of plant species (Glawe, 2008; Park and Wellings, 2012). Powdery mildew and rust fungi are obligate biotrophs; they are completely dependent on their host plant for growth and propagation, a fact that conditions significantly their lifestyle. A distinguishing feature of these obligate biotrophs is the formation of a specialized structure of parasitism, called the haustorium (Catanzariti *et al.*, 2007). Haustoria play an essential role in the acquisition of nutrients from plant cells and the deliverance of virulence factors, termed effectors (Weβling *et al.*, 2012). Fungal effectors are secreted proteins which, in the case of biotrophic fungi, appear to be responsible for suppression of the host immune response, modulation of the physiology or modification of the structure of host cells to provide a favourable environment for successful infection (Selin *et al.*, 2016). However, little is known about the role of powdery mildew and rust effectors in pathogenesis and their implications in host–pathogen interactions (Hacquard, 2014; Petre *et al.*, 2014).

In recent years, the increasing interest in the study of powdery mildew and rust effectors has uncovered the need to develop efficient methods to transform these families of obligate biotrophs. However, this task is challenging because of the non-amenability of these pathogens to traditional molecular genetics approaches, mainly as a result of difficulties in culturing these species *in vitro* (Martínez-Cruz *et al.*, 2017; Petre *et al.*, 2014). Despite the numerous studies on transformation in filamentous fungi, the stable transformation of powdery mildews and rusts remains unresolved (Chaure *et al.*, 2000; Christiansen *et al.*, 1995; Djulic *et al.*, 2011; Schillberg *et al.*, 2000; Vela-Corcía *et al.*, 2015; Webb *et al.*, 2006). A recently tested alternative to transform rust and powdery mildew fungi is so-called *Agrobacterium tumefaciens*-mediated transformation (ATMT) (Lawrence *et al.*,

2010; Martínez-Cruz *et al*., 2017). This bacterium introduces into the plant cell a DNA fragment, termed transfer DNA (T-DNA), together with a set of virulence proteins coded by Ti-plasmid-like VirD2 and VirE2 (Lai and Kado, 2000; Meyers *et al*., 2010; Pelczar *et al*., 2004). The set T-strand covered by VirE2 and linked to VirD2 is called the T-complex (Meyers *et al*., 2010). The T-complex travels through the plant cytoplasm to the nucleus, where the T-DNA can integrate into the host genome by random recombination (Meyers *et al*., 2010; Pelczar *et al*., 2004).

The ATMT technique has been widely employed in the transformation of different species of filamentous fungi, such as *Aspergillus awamori*, *Fusarium oxysporum* and *Penicillium digitatum* (Michielse *et al*., 2008, 2009 ; Wang and Li, 2008), leading to stable transformation. However, its use in rust and powdery mildew fungi is still far from routine. In the model flax rust fungus *Melampsora lini*, the method seems to provide stable integrations; however, the development of selection strategies based on fungicide or herbicide resistance is still needed (Lawrence *et al*., 2010). In the cucurbit powdery mildew fungus *Podosphaera xanthii*, the technique has been shown to be reproducible and reliable, but continues to result in a low number of transformants, as a consequence of the physical damage induced to conidia by co-incubation in an aqueous solution (Martínez-Cruz *et al*., 2017).

Host-induced gene silencing (HIGS) has become a reliable tool for the determination of the role of powdery mildew and rust effector candidates in the establishment of disease (Martínez-Cruz *et al*., 2018; Nowara *et al*., 2010; Panwar *et al*., 2013; Pliego *et al*., 2013). This method is based on the ability of the pathogen to take up, presumably via haustoria, harpin RNA or RNAi produced by plant cells after transformation with silencing constructs, which can subsequently induce gene silencing in haustorial cells (Govindarajulu *et al*., 2015; Panwar *et al*., 2013). HIGS results indicate the trafficking of RNA molecules from host plants into powdery mildew and rust fungi, and suggest an additional role for the haustorium in addition to the acquisition of nutrients and the delivery of effectors.

Based on these antecedents and the close relationship established between the powdery mildew haustoria and plant cells, we hypothesized that the haustorium could also act as a 'gateway' for the uptake of DNA as a novel route to introduce exogenous DNA into obligate biotrophs. To test our hypothesis, we used *P. xanthii* as a model powdery mildew species (Pérez-García *et al*., 2009) and *A. tumefaciens* as a vehicle to translocate DNA constructs into plant and haustorial cells. We agro-infiltrated several T-DNA constructs under the control of fungal promoters into melon cotyledons, which were subsequently inoculated with *P. xanthii* conidia. Our results conclusively showed the transfer of resistance markers and translational fusions from *A. tumefaciens* to *P. xanthii*. These results were further supported by the co-localization of *A. tumefaciens* VirD2 and a *P. xanthii* Rab protein into small vesicles of haustorial and hyphal cells, providing clues about the process of T-DNA uptake. The method, designated TGAT (transformation by growth onto agro-infiltrated tissues), is discussed as a potent tool for the development of genetic studies in powdery mildew fungi or other biotrophic fungal pathogens, whose host cells can easily be transformed by *A. tumefaciens*.

RESULTS

Acquisition of phenotypes by *P. xanthii* after growth onto agro-infiltrated tissues

Considering the intimate interaction established between the haustorium of powdery mildews and plant cells, and the efficiency of transformation of plant cells exhibited by *A. tumefaciens*, we decided to exploit these features to transform *P. xanthii*, using *Agrobacterium* to introduce T-DNA constructs (Fig. S1, see Supporting Information) into plant cells and, probably, also into haustorial cells. First, to demonstrate that the transformation of *P. xanthii* does not occur by the direct contact of *A. tumefaciens* cells with conidia, we conducted an analysis of the persistence of bacterial cells on the melon cotyledon surface. For this purpose, 24 h after treatment of the infiltrated cotyledons with cefotaxime, leaf samples were stained with 4′,6-diamidino-2-phenylindole (DAPI) and analysed by epifluorescence microscopy. We observed that agro-infiltrated melon cotyledons treated with cefotaxime did not present bacterial cells on the leaf surface (Fig. S2b, see Supporting Information). In contrast, agro-infiltrated melon cotyledons not treated with cefotaxime presented high accumulation of bacterial cells distributed following junction lines between epidermal cells (Fig. S2d, arrow).

After checking that cefotaxime kills *Agrobacterium* cells on the leaf surface, we proceeded to study the growth of *P. xanthii* on agro-infiltrated melon cotyledons. Thus, we initially agro-infiltrated two different T-DNA constructs harbouring two different selection markers, pPK2-hphgfp (hygromycin B resistance) and pPK2Tgfp (carbendazim resistance), in melon cotyledons and, as established in a previous study, the cotyledons were submerged in the corresponding selective agent solution after inoculation with powdery mildew conidia (Martínez-Cruz *et al*., 2017). Resistant colonies were obtained with both constructs at 10–12 days after pathogen inoculation (Fig. S3, see Supporting Information). However, hygromycin B-treated cotyledons suffered severe phytotoxicity damage (Fig. S3, arrowhead), which could negatively affect the transformation efficacy. Moreover, hygromycin B- and carbendazim-resistant colonies were small and did not cover completely the cotyledons, as occurs in the absence of selective agent or when a naturally carbendazim-resistant isolate is used (data not shown). Data obtained for each construct showed that, in all cases, transformed colonies were obtained; however, the number of carbendazim-resistant colonies was consistently more than twice that of hygromycin B-resistant colonies (Table 1). Furthermore, to analyse the stability of transformants, carbendazim- and hygromycin

Table 1 Transformation efficiency of *Podosphaera xanthii* after agro-infiltration of the plasmids, elimination of bacteria and inoculation of conidia.

Plasmids	Assays						Mean*
	1st	2nd	3rd	4th	5th	6th	
pPK2-hphgfp	1†	15	8	13	5	6	9.7 ± 1.62
pPK2Tgfp	26	27	18	11	24	19	20.8 ± 2.46

*Mean of transformed colonies obtained per assay ± standard error (SE).

†Number of colonies resistant to the corresponding fungicide obtained in each assay.

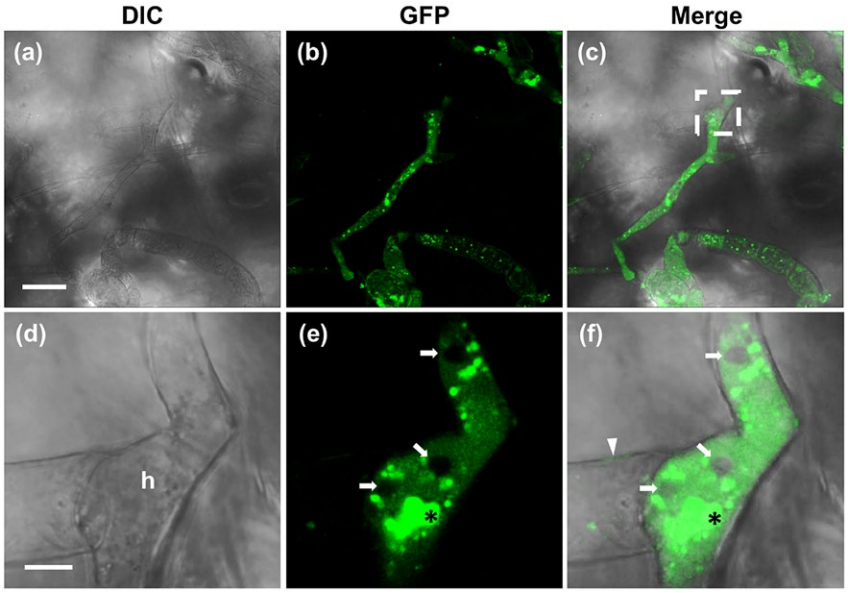

Fig. 1 Confocal laser scanning microscopy (CLSM) analysis of a *Podosphaera xanthii* hygromycin B-resistant colony obtained after transformation of a melon cotyledon with the transfer DNA (T-DNA) of pPK2-hphgfp and inoculation with *P. xanthii* conidia. (a–c) Presence of green fluorescent protein (GFP) signals in some hyphae. The overlay of differential interference contrast (DIC) and GFP images shows the irregular distribution of the fluorescence signal within the hyphae. Bar, 25 μm. (d–f) Details (white box) of one of the GFP-expressing hyphae (h) showing how GFP fluorescence is distributed in the cytoplasm of the fungal cell, presenting areas with no signal (arrows) and GFP agglomeration (asterisks). The overlay of the DIC and GFP images shows the GFP signal restricted to a transformed hypha, whereas an adjacent hypha does not present fluorescence (arrowhead). Scale bar, 5 μm.

B-resistant colonies were transferred to fresh melon cotyledons and treated with the corresponding selective agent. After 12 days of incubation, resistant colonies did not grow in the presence of selective pressure.

The T-DNA constructs used initially for *P. xanthii* transformation also harboured the *gfp* reporter gene. Before the analysis of green fluorescent protein (GFP) fluorescence in the resistant colonies, we analysed the transformation of the plant cells with the same constructs to rule out the possibility of GFP expression in the plant cells and the subsequent uptake of GFP by the pathogen. We transformed the plant cells with the binary vector pGWB6 which contains the *gfp* allele under the control of the 35S promoter (Fig. S1). The fluorescence signal was homogeneously distributed in the plant cells, but not in the fungi (Fig. S4b, see Supporting Information). In parallel, melon leaves infiltrated with the plasmid pPK2-hphgfp (Fig. S1), which contains the *gfp* gene under the control of the *gpdA* promoter from *Aspergillus nidulans*, did not present any fluorescence signal (Fig. S4d), which indicated that the plant cells do not express the GFP protein from the corresponding T-DNA construct.

After this test, we analysed resistant colonies for GFP fluorescence. We observed that the hyphae of *P. xanthii* that grew over the zones infiltrated with the pPK2-hphgfp plasmid presented profuse fluorescence signals that were not observed in the fraction of the fungal colonies that grew outside the limits of the infiltrated area (Fig. S5c, see Supporting Information). To observe in detail the pattern of fluorescence distribution, hygromycin B- and carbendazim-resistant colonies were analysed by confocal laser scanning microscopy (CLSM). In the transformants resistant to hygromycin B obtained with the T-DNA of the pPKT2-hphgfp plasmid, the GFP signal was observed in the cytoplasm of some hyphae (Fig. 1), but not in others. In addition, in the cytoplasm of

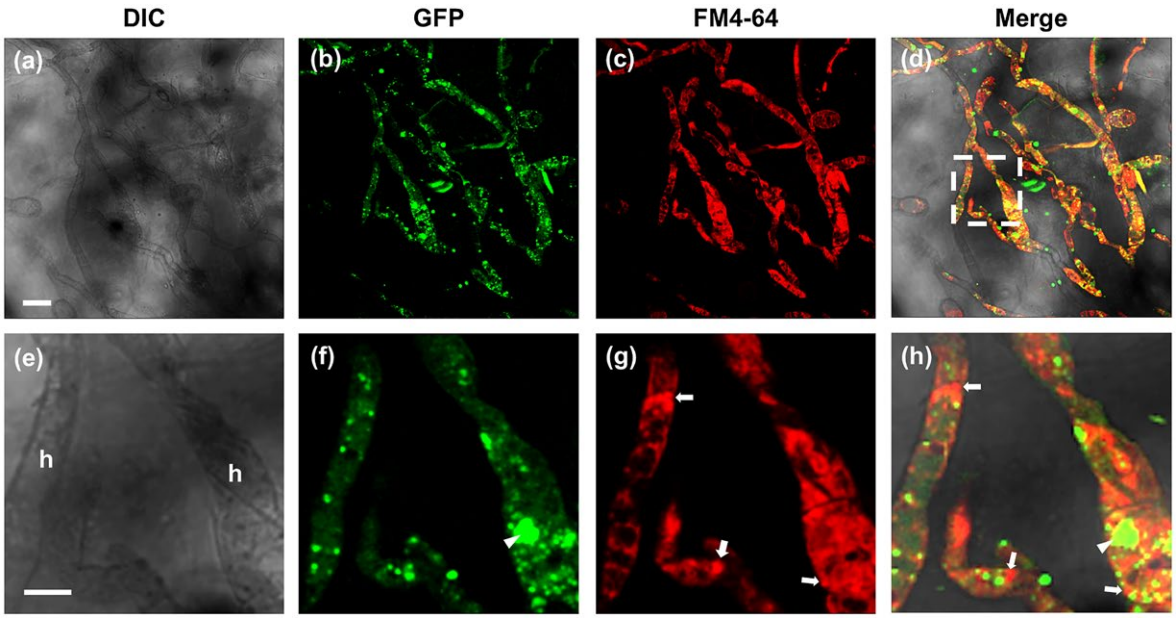

Fig. 2 Confocal laser scanning microscopy (CLSM) analysis of a *Podosphaera xanthii* carbendazim-resistant colony obtained after transformation of a melon cotyledon with the transfer DNA (T-DNA) of pPK2Tgfp and inoculation with *P. xanthii* conidia. (a–d) Presence of green fluorescent protein (GFP) signals along hyphae and staining of fungal membranes with FM4-64 membrane-specific dye. Scale bar, 25 μm. (e–h) Details (white box) of some GFP-expressing hyphae (h). GFP signals are present in the cytoplasm in the form of several agglomerations (arrowhead). FM4-64 staining reveals the presence of vesicles (arrows). Overlay of differential interference contrast (DIC) and CLSM images shows that the GFP signal does not co-localize with vesicles (arrows). Scale bar, 10 μm.

the transformants obtained with the T-DNA of the pPKT2-hphgfp plasmid, GFP aggregates and areas with no fluorescence signal could be observed (Fig. 1e,f). In the case of transformants resistant to carbendazim obtained with the T-DNA of the pPK2Tgfp plasmid (Fig. S1), a similar pattern of fluorescence distribution was observed (Fig. 2). Moreover, double staining with the FM4-64 dye showed that the GFP aggregates in the cytoplasm did not co-localize with vesicles (Fig. 2f,g). Indeed, some areas strongly stained with FM4-64 did not show a GFP signal (Fig. 2h).

Molecular analysis of *P. xanthii* transformants

The presence of T-DNA in putative *P. xanthii* transformant colonies was first evaluated by polymerase chain reaction (PCR) analysis using genomic DNA obtained from epiphytic biomass as a template. As expected from the phenotypic analysis, amplification signals of the expected size were obtained from all transformants, but not for untransformed colonies: 0.7 kb for the *hph* amplicon in the T-DNA of pPK2-hphgfp (Fig. S6a, see Supporting Information), and 0.8 kb for *gfp* and 2.2 kb for *tub2::gfp* amplicons in the T-DNA of pPKT2gfp (Fig. S6b). In the 2086 wild-type strains, the only signal of amplification was a 1.3-kb fragment obtained for the β-tubulin gene *Tub2* which was used as a positive control for amplification (Fig. S6a,b).

As a consequence of the small size of the resistant colonies, the amount of DNA that could be isolated was insufficient to carry out Southern blot analysis. Thus, we conducted thermal asymmetric interlaced-PCR (TAIL-PCR) analysis to identify the locus of integration of the T-DNA into the genome of four randomly selected *P. xanthii* transformants. After three rounds of PCR to enrich the amplification of the T-DNA border regions using three consecutive internal left and right border primers (LB1, LB2, LB3 or RB1, RB2, RB3), in combination with a degenerate primer (AD1), we obtained amplicons with different sizes (Fig. S7, see Supporting Information).

From the PCR products of the third round of TAIL-PCR, those with a difference of approximately 200 bp in comparison with the second-round products were isolated and sequenced (Fig. S7, white boxes). The analysis of the flanking sequences of the insertion sites of the T-DNA from the selected transformants revealed the loss of some nucleotides (3–88 nucleotides) at both borders, and the absence of similarity between them (Table S1, see Supporting Information), suggesting that T-DNA integration occurred randomly into the *P. xanthii* genome. In addition, BLAST searches revealed different integration sites for the transformants, including mostly intergenic regions in the proximity of several fungal hypothetical protein genes and an internal transcribed spacer (Table S2, see Supporting Information). Taken together, our results suggested that *A. tumefaciens* was indeed capable of transforming *P. xanthii* after infiltration into melon cotyledons.

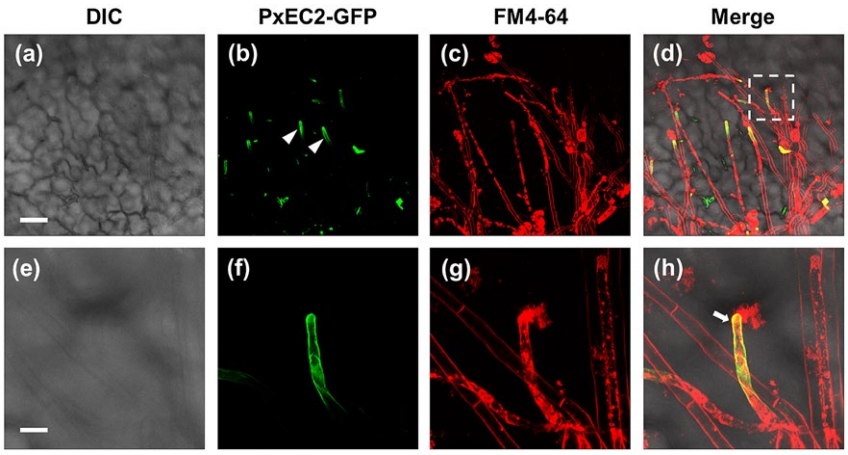

Fig. 3 Subcellular localization of the *Podosphaera xanthii* protein PxEC2. Melon cotyledons were transformed with the transfer DNA (T-DNA) of pPK2-PxEC2gfp and inoculated with *P. xanthii* conidia, and the fungal structures were examined by confocal laser scanning microscopy (CLSM). The photographs show the CLSM analysis of the periphery of the *P. xanthii* PxEC2-GFP transformant colony illustrated in Fig. S9. (a–d) The PxEC2-GFP signal is located at the hyphal tips (arrowheads). Scale bar, 50 μm. (e–h) Details (white box) of one of the PxEC2-GFP-expressing hyphal tips. The staining of membranes with FM4-64 dye (red) shows the co-localization of the PxEC2-GFP signal with the fungal membrane (arrows). Scale bar, 10 μm. DIC, differential interference contrast; GFP, green fluorescent protein. [Colour figure can be viewed at wileyonlinelibrary.com]

Subcellular localization of *P. xanthii* protein PxEC2

Once we had demonstrated that agro-infiltration could be an efficient system to transform *P. xanthii*, we considered the potential applications of this technique for powdery mildew research. An attractive application of the transformation of powdery mildew fungi is the study of the fungal genes putatively involved in the interaction with the host. Some of these genes encode putative secreted proteins containing cysteine-rich fungal extracellular membrane (CFEM) domains, which are believed to play a role in fungal pathogenesis (Kulkarni *et al.*, 2003). In *P. xanthii*, one of these genes is a possible homologue of the *Golovinomyces orontii EC2* gene (Fig. S8, see Supporting Information), which encodes a putative effector protein (Schmidt *et al.*, 2014; Vela-Corcía *et al.*, 2016). Considering the predicted location of these proteins at the fungal membrane, we designed an experiment to determine the subcellular localization of *P. xanthii* EC2 using a translational fluorescent fusion. For this purpose, we agro-infiltrated melon cotyledons with the plasmid pPK2-PxEC2gfp, a construct containing the translational fusion of *PxEC2* to the *gfp* gene (Fig. S1), and inoculated them with *P. xanthii* conidia. By epifluorescence microscopy, in the area agro-infiltrated with the plasmid pPK2-PxEC2gfp, the fungal colony showed an intense fluorescence, especially at the periphery, where fungal hyphae were actively growing (Fig. S9, arrowheads, see Supporting Information). By contrast, the central region of the colony, and hence the oldest, did not show fluorescence (Fig. S9, asterisk). The exact location of PxEC2-GFP was not obvious by epifluorescence microscopy; therefore, fluorescent colonies were analysed by CLSM. The PxEC2-GFP signal was only observed around hyphal tips (Fig. 3b–d, arrowheads). At higher magnification, GFP fluorescence appeared to be associated with the membrane of the fungal cells at the growing tip of the hypha, as indicated by the apparent co-localization of the GFP signal with the red signal corresponding to the membrane-specific dye FM4-64 (Fig. 3f–h, arrowhead). In conclusion, using this method, we successfully expressed a fusion protein in *P. xanthii* and observed a fluorescence signal distribution completely different from that observed previously with the other T-DNA constructs, which reinforced the robustness of the transformation technique.

Subcellular localization of *A. tumefaciens* VirD2 protein in the nucleus and endosomes

The results of the phenotypic and molecular characterization of *P. xanthii* transformants suggested that, indeed, *A. tumefaciens* was able to translocate the T-DNA into fungal cells. It is well known that T-DNA enters the plant cell using a type IV secretion system (T4SS) involving the production of a T-pilus; however, what is the mechanism that allows the entry of T-DNA into the fungal cells in this case? To address this question, we first expressed the *A. tumefaciens* protein VirD2, the protein responsible for guiding the T-DNA to the nucleus, fused to the enhanced GFP (eGFP) protein (Fig. S1). Prior to the agro-infiltration of melon cotyledons, we tested the plasmid pGWB6-egfpVirD2 for fungal transformation to rule out the possibility of the expression of the eGFP-VirD2 fusion by fungal cells. After direct transformation of *P. xanthii* conidia by ATMT (Martínez-Cruz *et al.*, 2017), colonies transformed with the T-DNA of pGWB6-egfpVirD2, which contain the egfp-VirD2 fusion under the control of the 35S promoter, did not present any fluorescence signal (Fig. S10b, see Supporting Information). Conversely, *P. xanthii* colonies transformed with

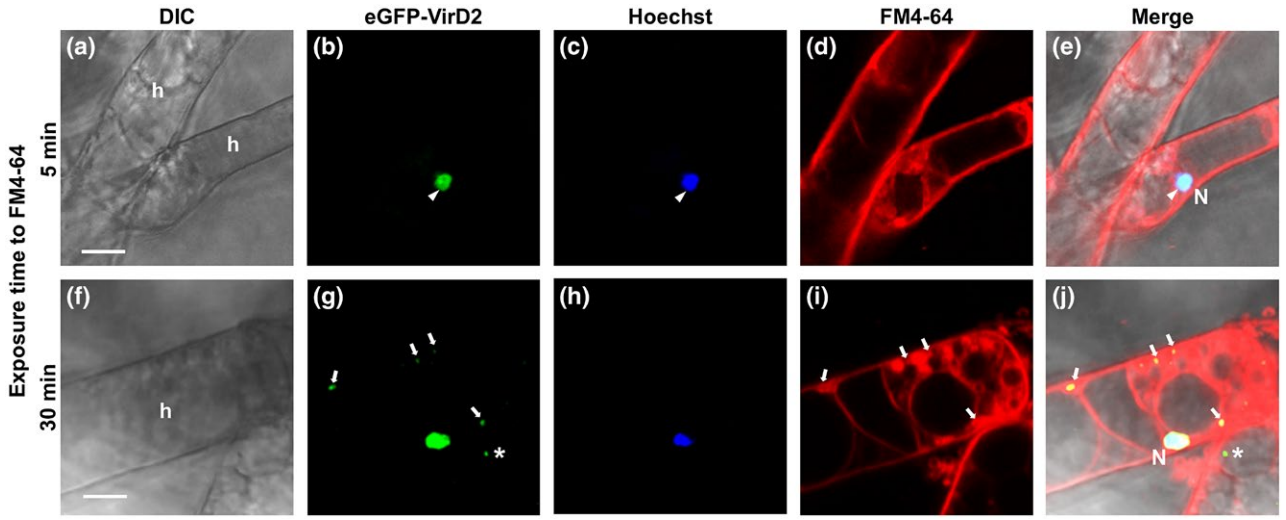

Fig. 4 Subcellular localization of the *Agrobacterium* protein VirD2 in *Podosphaera xanthii*. Melon cotyledons were agro-infiltrated with pGWB6-VirD2 and inoculated with *P. xanthii* conidia, and the fungal structures were examined by confocal laser scanning microscopy (CLSM). For the visualization of nuclei and membranes of *P. xanthii* hyphal cells (h), staining with Hoechst (blue) and FM4-64 (red) dyes, respectively, was performed. (a–e) After 5 min of exposure to FM4-64, only the fluorescence signals of eGFP-VirD2 (green) and nucleus (N) co-localized (arrowheads). (f–j) After a 30-min exposure to FM4-64, vesicles (arrows) and vacuoles (asterisk) were visible. Under these conditions, the eGFP-VirD2 signal was found to co-localize with the nucleus (N) and with putative vesicles (arrows). Furthermore, the eGFP-VirD2 signal was also observed in a large vacuole (asterisk). Scale bars, 5 μm. DIC, differential interference contrast; GFP, green fluorescent protein. [Colour figure can be viewed at wileyonlinelibrary.com]

the T-DNA of pPK2-hphgfp, which contains the *gfp* gene under the control of the *gpdA* promoter from *A. nidulans*, presented a homogeneous fluorescence signal (Fig. S10d).

After this check, the construct pGWB6-egfpVirD2 was agro-infiltrated into melon cotyledons, which were subsequently inoculated with *P. xanthii* conidia. Five days after inoculation, we observed a fluorescence signal in fungal colonies by epifluorescence microscopy. As observed for the other constructs, only that part of the colony that grew above the infiltrated area emitted eGFP fluorescence, which was distributed irregularly, accumulating as foci in the fungal hyphae (Fig. S11, asterisks, see Supporting Information). To determine the exact location of the fluorescence signal, we carried out CLSM analysis. The eGFP signal was restricted to a small area of the haustorium, presumably the nucleus (Fig. S12b,c, arrowheads, see Supporting Information). To confirm the nuclear localization of the eGFP-VirD2 signal, double staining with the DNA-specific dye Hoechst (blue) and the membrane-specific dye FM4-64 (red) was performed. By this approach, localization of the eGFP-VirD2 signal in the nucleus of the fungal cell was demonstrated (Fig. 4a–e, arrowhead). Longer exposure to FM4-64 allowed the staining of other membranous structures, such as small vesicles, which eventually also contained eGFP-VirD2-associated signal (Fig. 4f–j, arrows). Moreover, eGFP-VirD2 signal was also found to be associated with a large vacuole (Fig. 4g,j, asterisks).

The association of the eGFP-VirD2 signal with small vesicles was further corroborated by the co-localization of *Agrobacterium* VirD2 with fungal Rab5, a protein that localizes in early endosomes. For this purpose, the translational fusion of cyan fluorescent protein (CFP) to PxRab5 was constructed, yielding the plasmid pPK2-cfpPxRab5 (Fig. S1). In this experiment, pPK2-cfpPxRab5 and pGWB6-egfpVirD2 plasmids were co-infiltrated into melon cotyledons, which, once again, were inoculated with *P. xanthii* conidia. After incubation, hyphal and haustorial cells were isolated and analysed by CLSM. As anticipated, in haustorial and hyphal cells, the signal corresponding to eGFP-VirD2 (green) was found to co-localize with the signal associated with CFP-PxRab5 (cyan) (Figs 5a and S13, see Supporting Information). Moreover, we observed some eGFP-VirD2 signal co-locating with an intense CFP-PxRab5 signal around the extrahaustorial membrane (Fig. 5a, arrowhead). The co-localization was confirmed by signal quantification, showing that the relative intensities of CFP and eGFP in the vesicles of haustorial and hyphal cells were identical (Fig. 5b). Taken together, these results conclusively demonstrated that the *Agrobacterium* transformation machinery was indeed responsible for the transformation of the fungal cells, and suggested endocytosis by the haustorium as the mechanism of VirD2 uptake and, hence, of T-DNA uptake. Furthermore, the observation of specific signals associated with two different translational fusion proteins (PxEC2-GFP and CFP-PxRab5) confirmed the reliability and robustness of the transformation method, as well as its potential for different applications in powdery mildew research.

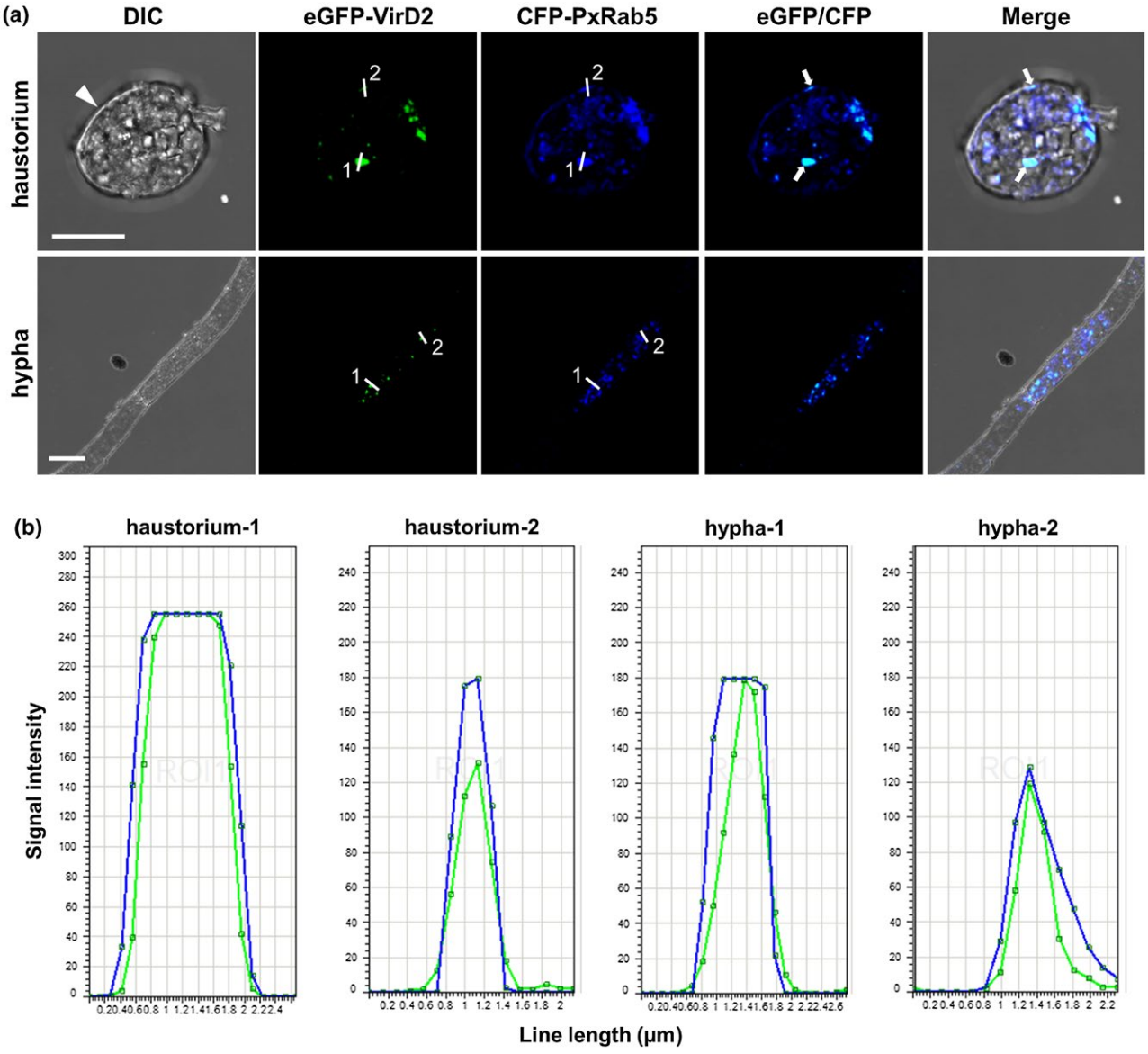

Fig. 5 Subcellular localization of the *Agrobacterium* protein VirD2 and the endocytic vesicle-associated fungal protein Rab5 in *Podosphaera xanthii* transformants. Melon cotyledons were co-agro-infiltrated with pGWB6-egfpVirD2 and pPK2-cfpRab5 containing the translational fusions eGFP-VirD2 and CFP-Rab5, respectively, and inoculated with *P. xanthii* conidia; the fungal structures were examined by confocal laser scanning microscopy (CLSM). (a) CLSM analysis of eGFP-VirD2 (green) and CFP-Rab5 (blue) fusions in *P. xanthii* haustorial and hyphal cells. Top row: intact isolated haustorium with extrahaustorial membrane (arrowhead) showing the co-localization of eGFP-VirD2 and CFP-Rab5 signals (arrows). Scale bar, 5 μm. Bottom row: isolated hypha also showing the co-localization of the eGFP-VirD2 and CFP-Rab5 signals. Scale bar, 20 μm. (See Fig. S13 for additional haustorial and hyphal cells.) (b) Signal intensity of eGFP-VirD2 and CFP-PxRab5 in putative vesicles of haustorial and hyphal cells. Cross-sectional lines (1 and 2) were drawn over putative vesicles of haustorial and hyphal cells; the signal was quantified using the Leica Microsystems LAS AF image analysing program. The eGFP-VirD2 and CFP-PxRab5 signals show overlapping intensity, confirming the presence of VirD2 in, presumably, endocytosis vesicles. CFP, cyan fluorescent protein; DIC, differential interference contrast; GFP, green fluorescent protein. [Colour figure can be viewed at wileyonlinelibrary.com]

DISCUSSION

To date, a number of methods for the transformation of filamentous fungi have been developed (Jiang *et al.*, 2013). Some have been tested in powdery mildews, but, unfortunately, the transformation is unstable and the number of transformants is, if any, very low (Martínez-Cruz *et al.*, 2017). The problematic handling of these fungi, together with the fragility of their spores, led us to consider alternative ways to introduce exogenous DNA. Powdery mildew fungi establish an intimate relationship with their host through the haustorium (Martínez-Cruz *et al.*, 2014).

The haustorium mediates the exchange of diverse factors with the plant, including the uptake of small RNAs; thus, we reasoned that this uptake activity could be exploited to efficiently transform *P. xanthii* with exogenous DNA (Martínez-Cruz *et al.*, 2018; Panwar *et al.*, 2013; Pliego *et al.*, 2013). Thus, we conceived agro-infiltration as a method to transform plant cells and, ideally, haustorial cells, using a variety of vectors previously employed to transform *P. xanthii* conidia with *A. tumefaciens* (Martínez-Cruz *et al.*, 2017). By doing so, we reasoned that the T-DNA contained in the plant cytoplasm could somehow be taken up by *P. xanthii* haustoria. Our results show that *P. xanthii*, and perhaps other haustorium-forming fungal pathogens, can be easily transformed by growing them on agro-infiltrated tissues.

The promiscuous infectivity of *A. tumefaciens* might lead to the argument that direct infection of *P. xanthii* conidia is responsible for the transformation. However, in our transformation method, cotyledons were treated with cefotaxime prior to powdery mildew inoculation to kill *Agrobacterium* cells, thus preventing the direct transformation of conidia. In addition, after infiltration, most *Agrobacterium* cells are restricted to the apoplast (Goulet *et al.*, 2010), whereas *P. xanthii* haustoria develop within epidermal cells (Martínez-Cruz *et al.*, 2014); therefore, direct contact between *Agrobacterium* and fungal cells is unlikely.

Compared with the ATMT method, in which *Agrobacterium* transforms conidia (Martínez-Cruz *et al.*, 2017), the number of *P. xanthii* colonies resistant to either carbendazim or hygromycin B obtained by TGAT was 10 times higher, probably because of the non-aggression towards the fungus. In the ATMT method, conidia are exposed to the stress caused by the co-cultivation with *A. tumefaciens* in an aqueous solution (Martínez-Cruz *et al.*, 2017). In our study, we also observed a consistently higher number of transformants (twice) resistant to carbendazim than to hygromycin B. This is a recurrent finding (Martínez-Cruz *et al.*, 2017; Vela-Corcía *et al.*, 2015) that led us to propose that the loss of viability of the plant cells inflicted by hygromycin B was the most probable explanation of the reduced number of transformants, a fact that will prevent its use in further studies.

Some of the transformants were analysed further, both phenotypically and molecularly. We demonstrated that, apart from showing antifungal resistance, these transformants expressed GFP in a robust manner. In addition, molecular analyses showed that these transformants contained the artificial constructs: first, by PCR analysis to detect the constructs in fungal DNA and, second, by TAIL-PCR analysis to obtain the T-DNA flanking regions. The sequence analysis confirmed the existence of different genomic T-DNA integration sites for each transformant. Interestingly, and as observed previously (Martínez-Cruz *et al.*, 2017), most of the integration sites seemed to be intergenic regions. Powdery mildews are obligate parasites which have lost many genes during evolution and host adaptation, probably keeping essential ones (Spanu *et al.*, 2010). It is possible that many T-DNA insertions occur, but most may cause fitness cost penalties, and only those inserted in non-coding regions develop. Altogether, our results indicated that *P. xanthii* was able to take the T-DNA from the plant cell cytoplasm and integrate it into the genome. Unfortunately, transformation was found to be unstable, as the transformants could not be cultivated further. Probably, as documented previously for *P. xanthii* transformants obtained by ATMT of conidia, the T-DNAs are excised from the genome (Martínez-Cruz *et al.*, 2017).

Effector biology is a growing field and is one of the main reasons for the investment of efforts to develop a reliable method for the transformation of powdery mildew fungi. Although there are alternative systems, such as HIGS, for the functional analysis of powdery mildew effector candidate genes (Ahmed *et al.*, 2015; Martínez-Cruz *et al.*, 2018; Pennington *et al.*, 2016; Pliego *et al.*, 2013; Whigham *et al.*, 2015), the localization and secretion of these candidates remain a problem. To test the reliability of the TGAT method, in this work, we also aimed to localize subcellularly a powdery mildew protein as a translational fusion. For this purpose, we chose the CFEM domain-containing protein PxEC2. The CFEM domain proteins are membrane-associated proteins (Kulkarni *et al.*, 2003). Such evidence has been corroborated in a previous study, where a CFEM domain protein from *Magnaporthe oryzae* was located in the fungal membrane (Ramanujan *et al.*, 2013). The predicted subcellular location of PxEC2 as a CFEM domain protein was the reason why we selected this protein. As expected, the PxEC2-GFP signal co-located with the membrane of *P. xanthii*. Moreover, the PxEC2-GFP signal was observed in the tips of the growing hyphae of the outer parts of the colony, as also described in *M. oryzae* (Ramanujan *et al.*, 2013).

It is well established how T-DNA enters the plant cell. However, how does the T-DNA transit from the plant cytoplasm to finally reach the fungal cells? The *Agrobacterium* Vir proteins VirD2 and VirE2 are the accompanying proteins of T-DNA and the proteins responsible for driving the T-DNA to the nucleus (Bhattacharjee *et al.*, 2008; Eckardt, 2004; Pelczar *et al.*, 2004). To determine the mechanisms of entry of T-DNA into the fungal cell, we decided to study the subcellular localization of the VirD2 protein in *P. xanthii*. For this study, we carried out the expression of the eGFP-VirD2 translational fusion in melon cotyledon cells, because it is known that the GFP-VirD2 fusion is unable to cross the T-pilus formed by *A. tumefaciens* because of its excessive size, being retained in the bacterial cytoplasm (Bhattacharjee *et al.*, 2008). By CLSM analysis, we detected the eGFP-VirD2 signal in the nucleus of fungal cells and in some putative vesicles. Further, the direct transformation of conidia of *P. xanthii* by ATMT showed that the T-DNA of pGWB6-egfpVirD2 is not functional in the fungus, and so the eGFP-VirD2 fusion is taken up by the pathogen, thus supporting our original idea that the *P. xanthii* haustorium would be able to take up the T-complex from the plant cytoplasm. However, how can the T-complex be taken up

by the haustorium? The two possible methods of entry of the T-complex could be those previously described for the uptake of molecules by fungi, that is, osmotrophic feeding and endocytosis (Higuchi *et al.*, 2006; Michael *et al.*, 2009; Read and Kalkman, 2003; Richards and Talbot, 2013).

In a previous study, the transcriptomic analysis of *P. xanthii* epiphytic structures revealed the presence of Rab transcripts, which encode proteins dedicated to endocytosis (Vela-Corcía *et al.*, 2016). Therefore, to test the 'endocytosis hypothesis', we carried out the localization of VirD2 and Rab proteins. Rab proteins are small monomeric GTPases that regulate many steps of membrane trafficking, including vesicle formation, vesicle movement and recruitment of effectors (Jovic *et al.*, 2010; Stenmark, 2009). Rab5 is the most extensively analysed Rab protein of the early endocytic pathway and regulates the entry of the cargo from the plasma membrane to the early/sorting endosomes (Cavalli *et al.*, 2001; Jovic *et al.*, 2010). The co-localization of eGFP-VirD2 and CFP-PxRab5 fusions in haustorial and hyphal vesicles, observed by confocal microscopy, supported the 'endocytosis hypothesis'. In addition, it was observed that Rab5 was abundantly present in the haustoria, the organs responsible for the nutrient uptake from the plant cell, and, especially, in the extrahaustorial membrane. However, it is interesting to note that not all Rab5-containing vesicles showed eGFP-VirD2 signals. This

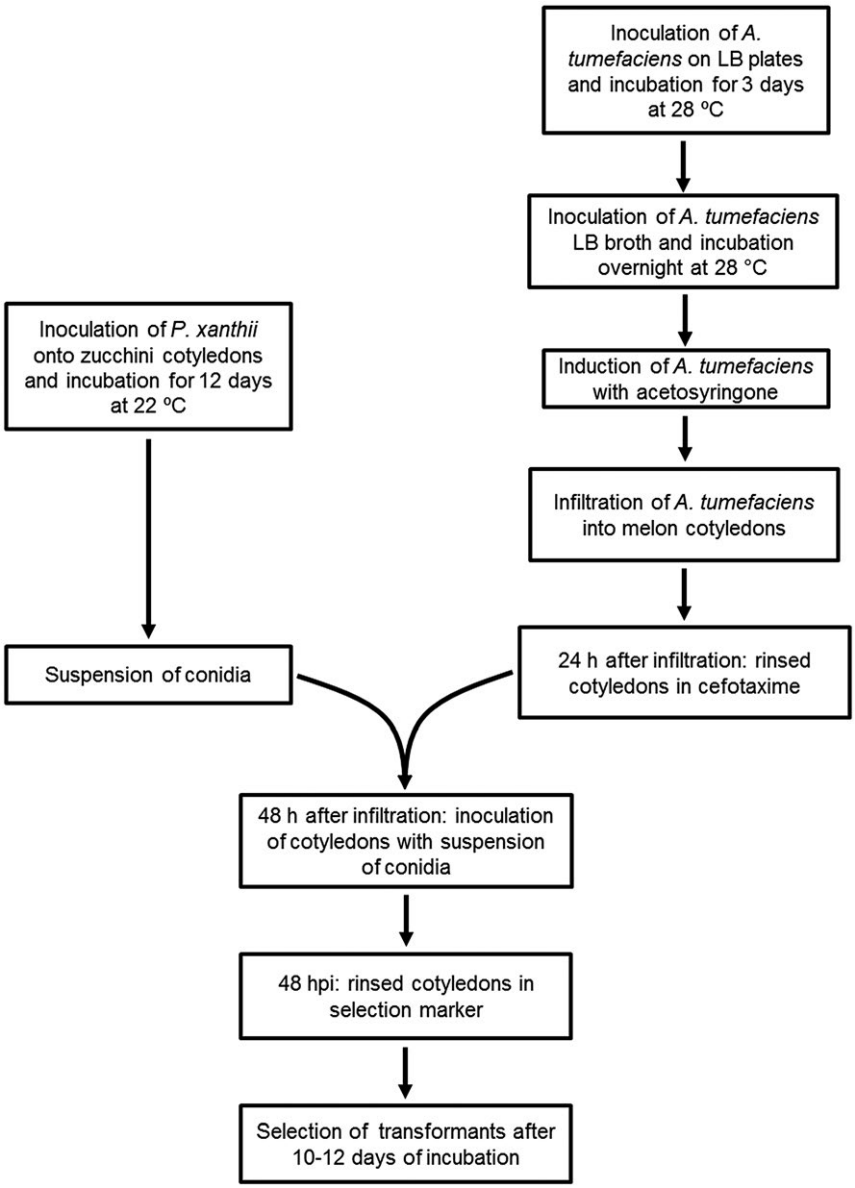

Fig. 6 Flow diagram of the method for the transformation of *Podosphaera xanthii*, designated as 'transformation by growth onto agro-infiltrated tissues' (TGAT). hpi, hours post-inoculation; Lysogeny Broth (LB).

was expected because not all of these vesicles contain the VirD2 protein. Moreover, we also observed the co-localization of VirD2 and Rab5 fusion signals in the extrahaustorial membrane, which suggests that VirD2, and hence the T-complex, is preferentially taken up by the haustorium. In the light of these results, we provide a model that proposes endocytosis by the haustorium as the most probable method of T-complex capture from the plant cytoplasm (Fig. S14, see Supporting Information). Once internalized by the haustorial cell, the T-DNA may follow two alternative pathways: integration into the fungal genome of haustorial or hyphal cells, or degradation in the fungal vacuoles. The results presented here demonstrate the transfer of genetic material from *A. tumefaciens* to an obligate biotrophic fungus, in a process facilitated by the plant cell, in which the haustorium seems to play a pivotal role.

CONCLUSIONS

We have designed a novel transformation method for powdery mildew fungi which relies on the use of *Agrobacterium* to transform the pathogen simply by its growth on previously agro-infiltrated tissues (Fig. 6). Unlike previous methods developed for powdery mildews, we demonstrate the robustness and reproducibility of our method by assessing different constructs including translational fusions and transforming the cucurbit powdery mildew pathogen *P. xanthii*. As *Agrobacterium* naturally has a wide host range in plants, primarily dicot species (Pitzschke, 2013), we anticipate that TGAT is likely to work for other powdery mildews and other haustorium-forming fungal pathogens, whose hosts are capable of being transformed by *Agrobacterium*. The haustorium, essential in their lifestyle, mediates the uptake of nutrients and the secretion of fungal effectors but, as shown in this work, may also represent the 'entrance door' for foreign genetic material in obligate biotrophs.

EXPERIMENTAL PROCEDURES

Fungi, plants and bacteria

The *P. xanthii* isolate 2086 was cultured and maintained on zucchini (*Cucurbita pepo* L.) cotyledons cv. Negro Belleza (Semillas Fitó, Barcelona, Spain) in an 8-cm Petri dish under a 16-h light/8-h dark cycle at 22 °C for 1 week (Álvarez and Torés, 1997). For agro-infiltration experiments, melon (*Cucumis melo* L.) cotyledons cv. Rochet (Semillas Fitó) were used. Zucchini and melon seedlings were grown from seeds previously germinated in the dark, in a growth chamber with a 16-h light/8-h dark cycle at 25 °C until use. The *Escherichia coli* strain DH5α, used in the construction, propagation and amplification of the vectors, was grown at 37 °C in LB medium containing kanamycin (50 μg/mL). The *A. tumefaciens* strains LBA4404 and C58C1, used in agro-infiltration assays, were grown at 28 °C in LB medium containing rifampicin (50 μg/mL) and kanamycin (50 μg/mL). The fungicides hygromycin B and carbendazim were used at 100 μg/mL and 600 μg/mL, respectively, when required.

Construction of binary vectors

The T-DNAs of the binary vectors used in this study are shown in Fig. S1. The primer sequences used in this work are displayed in Table S3 (see Supporting Information). The plasmids pPK2-hphgfp and pPK2Tgfp have been described previously (Martínez-Cruz *et al.*, 2017). The plasmid pPK2-PxEC2gfp contains the translational fusion of the CFEM domain protein PxEC2 from *P. xanthii* (ACCN KY979944) (Vela-Corcía *et al.*, 2016) to GFP. To build the pPK2-PxEC2gfp plasmid, the *PxEC2* gene was amplified from *P. xanthii* cDNA using the primer pair PxEC2-F and PxEC2-R. Total RNA was isolated from melon cotyledons containing 9-day-old *P. xanthii* colonies using a TRI Reagent® RNA isolation system (Sigma-Aldrich, Steinheim, Germany). To remove DNA contamination, a DNA TURBO DNA-free kit® (Ambion, Barcelona, Spain) was used. cDNAs were then synthesized using Superscript® III Reverse Transcriptase (Invitrogen, Madrid, Spain) and Oligo dT(20) primer (Invitrogen). The *PgpdA* promoter and the *gfp* gene were separately amplified from pPK2-hphgfp vector using the primer pairs PgpdA-F/PgpdA-R-PxEC2 and gfp6F1-PxEC2/gfp6R1-ApaI, respectively, and fused to the *PxEC2* cDNA fragment by overlapping PCR using the primer pair PgpdA-F and gfp6R1-ApaI. The 3.4-kb fragment was digested with *Apa*I and *Kpn*I restriction enzymes and cloned into the same cut of pPK2-hphgfp.

The pPK2-cfpRab5 vector contains a sequence consisting of the *P. xanthii Rab5* cDNA (ACCN KY979945) encoding a small GTP-binding protein that regulates membrane trafficking fused to the *cfp* gene. To construct the pPK2-cfpRab5 plasmid, the *Rab5* allele from isolate 2086 was amplified using the primer pair Rab5-F and Rab5-R. The *PgpdA* promoter was amplified from pPK2-hphgfp as indicated above, and the *cfp* allele was amplified from pKM008 with the primer pair CFP-F and CFP-R. These fragments were fused to the DNA fragment of the *Rab5* allele by overlapping PCR using the primers PgpdA-F and Rgfp6-ApaI. The purified 3.5-kb fragment was digested with *Apa*I and *Kpn*I restriction enzymes and cloned into the cut vector pPK2-hphgfp.

The pPK2-PxEC2gfp and pPK2-cfpRab5 plasmids were checked by PCR and digestion, and cloned and maintained in *E. coli* DH5α. The pPK2-hphgfp vector was transferred to *A. tumefaciens* LBA4404, and pPK2Tgfp, pPK2-PxEC2gfp and pPK2-cfpRab5 were separately transferred to *A. tumefaciens* C58C1.

For the subcellular localization of the *A. tumefaciens* VirD2 protein, the pGWB6-egfpVirD2 vector was constructed using the Gateway™ Cloning system (Invitrogen). The vector contains the translational fusion of e*gfp* to *VirD2*. To build the plasmid,

the *VirD2* gene was amplified using the primers VirD2donor-F and VirD2donor-R with the corresponding attB1 and attB2 tails from *A. tumefaciens* C58C1. The resulting PCR product was re-amplified with attB1 and attB2 primers to add the att sequences. The final PCR product was introduced into the donor vector pDONR207 (Invitrogen) by BP reaction. Then, the PCR product was integrated into the binary vector pGWB6 (Nakagawa *et al.*, 2007) by LR reaction (Invitrogen). Recombination reactions were performed as described in the manufacturer's instructions (Invitrogen). The recombinant plasmid was introduced into *E. coli* DH5α and verified by PCR and digestion. The resulting pGWB6-egfpVirD2 vector was finally transferred to *A. tumefaciens* C58C1 by electroporation.

Agro-infiltration assay

For this assay, 5-mL cultures of *A. tumefaciens* LBA4404 or C58C1, harbouring the corresponding T-DNA construct, were grown overnight at 28 °C in LB broth containing rifampicin (50 μg/mL) and kanamycin (50 μg/mL) in an orbital shaker at 200 rpm. Subsequently, the cultures were prepared and infiltrated into melon cotyledons as described previously (Martínez-Cruz *et al.*, 2018).

Twenty-four hours after infiltration, the cotyledons were rinsed with cefotaxime (200 μg/mL) to kill *Agrobacterium* cells (Dubresson *et al.*, 2008). Twenty-four hours later, the leaves were inoculated by pulverization with fresh suspensions of *P. xanthii* conidia (10^6 spores/mL). For the selection of *P. xanthii* transformants, 48 h after the inoculation of conidia, the leaves were immersed in solutions of hygromycin (100 μg/mL) or carbendazim (600 μg/mL), according to plasmid-encoded resistance. The plants were maintained under a 16-h light/8-h dark cycle at 25 °C for 10–12 days to allow the development of transformants.

Epifluorescence microscopy

Fluorescence analyses of agro-infiltrated melon cotyledons and transformed *P. xanthii* colonies were performed using a Nikon AZ-100 epifluorescence microscope (Nikon, Tokyo, Japan) equipped with filters suitable for the analysis of GFP and ultraviolet (UV). For the analysis of the GFP fluorescence, the samples of either agro-infiltrated melon cotyledons or *P. xanthii* transformed colonies were examined under a GFP filter and excited at wavelengths of 460–500 nm and a fixed exposure of 2 s. The UV fluorescence analysis was used to evaluate the persistence of *A. tumefaciens* cells on the leaf surface or to observe fungal growth. For the latter, cotyledon discs were stained with aniline blue and calcofluor white as described previously (Martínez-Cruz *et al.*, 2014). For the observation of bacteria, 24 h after cefotaxime treatment, cotyledon discs were stained with a 10 μg/mL solution of DAPI. In both cases, the samples were examined under a UV filter and excited at wavelengths of 330–380 nm and a fixed exposure of 2 s. All of the images were captured with a Nikon digital Slight DS-5Mc camera attached to the microscope, using Nis-Elements software (Nikon), and were processed using Adobe Photoshop CS5 (Adobe Systems, San José, CA, USA).

Molecular analysis of transformants

Genomic DNA from potential *P. xanthii* transformants was isolated following a modified alkaline lysis method (Kieleczawa, 2006). Epiphytic fungal biomass was removed from cotyledons and loaded into 25 μL of 0.25 N KOH for 10 min at 90 °C. After this incubation, the solution was neutralized using 25 μL of neutralization solution (0.5 M Tris-HCl, pH 8.0) for 10 min at 90 °C. Finally, the DNA was separated using 50 μL of a chloroform/isoamyl alcohol (24 : 1) gradient in the aqueous phase.

The presence of T-DNA in the genomic DNA preparations was first analysed by PCR. To analyse the transformants obtained with the T-DNA of pPK2-hphgfp, fragments of the *gfp* and *hph* marker genes were amplified using the primer pairs gfp6F1/gfp6R1 and hphF1/hphR1 (Table S3), respectively. For transformants obtained with the T-DNA of pPK2Tgfp, the primer pairs Tub-F/gfp6R1 and gfp6F1/gfp6R1 (Table S3) were used to amplify the fragment *tub2-gfp*. The amplification conditions were as follows: 95 °C for 2 min, followed by 35 cycles of 95 °C for 30 s, 55 °C for 1 min and 72 °C for 4 min, with a final extension at 72 °C for 10 min. Finally, the PCR products were electrophoresed in 1% agarose gels and visualized under UV light.

To analyse the flanking regions of the T-DNA insertions, TAIL-PCR was performed as described previously (Martínez-Cruz *et al.*, 2017).

Confocal laser scanning microscopy (CLSM)

The subcellular localization of the translational fusions PxEC2-GFP, eGFP-VirD2 and CFP-PxRab5 was studied by CLSM analysis. The GFP and CFP proteins were excited with 488- and 405-nm laser lines, and their fluorescence was detected at 495–530-nm and 460–485-nm bandpasses, respectively. The nuclei of fungal cells were visualized using a 2 μg/mL solution of Hoechst dye (blue) (Thermo Scientific, Barcelona, Spain) in phosphate-buffered saline (PBS). Fungal membranes were selectively stained using a 0.02 mg/mL solution of FM4-64 dye (red) (Sigma-Aldrich, Steinheim, Germany) in PBS. The samples were observed using a Leica SP5 II confocal microscope (Leica Microsystems, Wetzlar, Germay). Bright field images were made using the transmission channel. All images were observed using a 63× oil-immersion objective and were processed using Leica LAS AF software LCS Lite (Leica Microsystems).

Isolation of hyphal and haustorial cells

To facilitate the observation in detail of *P. xanthii* hyphal and haustorial cells by CLSM, these fungal structures were isolated from transformed colonies at 72 h after transformation. Briefly, hyphae were carefully separated from the infected cotyledon surface using a spatula and quickly resuspended in chilled PBS. For the isolation of haustoria, melon cotyledons with transformed colonies were homogenized and processed essentially as described previously (Martínez-Cruz *et al.*, 2014) with the following modifications. After filtering the homogenate through an 11-μm nylon filter, the suspension was centrifuged at 6500 g for 10 min at 4 °C and the supernatant was discharged. The resulting pellet, enriched in haustoria, was then resuspended in 5 mL of chilled PBS.

ACCESSION NUMBERS

Sequence data from this article can be found in the GenBank/EMBL databases under the following accession numbers: PxEC2, KY979944; PxRab5, KY979945.

ACKNOWLEDGEMENTS

We thank Irene Linares (University of Malaga, Spain) for excellent technical assistance. We are grateful to Dr Tsuyoshi Nakagawa (Shimane University, Japan) for kindly providing the plasmid pGWB6. This work was supported by grants from the 'Agencia Estatal de Investigación (AEI)' (AGL2013-41939-R and AGL2016-76216-C2-1-R), both co-financed by FEDER funds (European Union). J.M.-C. was supported by a PhD fellowship (BES-2011-046757) from the former 'Ministerio de Ciencia e Innovación (MICINN)'. D.R. was funded by the 'Ramón y Cajal' program (RyC-2011-080605) from the 'Ministerio de Economía y Competitividad (MINECO)'. The authors declare no conflicts of interest.

REFERENCES

Ahmed, A.A., Pedersen, C., Schultz-Larsen, T., Kwaaitaal, M., Jørgensen, H.J. and Thordal-Christensen, H. (2015) The barley powdery mildew candidate secreted effector protein CSEP0105 inhibits the chaperone activity of a small heat shock protein. *Plant Physiol.* **168**, 321–333.

Álvarez, B. and Torés, J.A. (1997) Cultivo in vitro de *Sphaerotheca fuliginea* (Schlecht. ex. Fr.), efecto de diferentes fuentes de carbón sobre su desarrollo. *Bol. San. Veg. Plagas,* **23**, 283–288.

Bhattacharjee, S., Lee, L.Y., Oltmanns, H., Cao, H., Veena Cuperus, J. and Gelvin, S.B. (2008) IMPa-4, an *Arabidopsis* importin α isoform, is preferentially involved in *Agrobacterium*-mediated plant transformation. *Plant Cell,* **20**, 2661–2680.

Catanzariti, A.M., Dodds, P.N. and Ellis, J.G. (2007) Avirulence proteins from haustoria-forming pathogens. *FEMS Microbiol. Lett.* **269**, 181–188.

Cavalli, V., Corti, M. and Gruenberg, J. (2001) Endocytosis and signaling cascades: a close encounter. *FEBS Lett.* **498**, 190–196.

Chaure, P., Gurr, S.J. and Spanu, P. (2000) Stable transformation of *Erysiphe graminis* an obligate biotrophic pathogen of barley. *Nature*, **18**, 205–207.

Christiansen, K.S., Knudsen, S. and Giese, H. (1995) Biolistic transformation of the obligate plant pathogenic fungus *Erysiphe graminis* f. sp. *hordei*. *Curr. Genet.* **29**, 100–102.

Djulic, A., Schmid, A., Lenz, H., Sharma, P., Koch, C., Wirsel, S.G.R. and Voegele, R.T. (2011) Transient transformation of the obligate biotrophic rust fungus *Uromyces fabae* using biolistics. *Fungal Biol.* **115**, 633–642.

Dubresson, R., Kravchuk, Z., Neuhaus, J.M. and Mauch-Mani, B. (2008) Optimisation and comparison of transient expression methods to express the green fluorescent protein in the obligate biotrophic oomycete *Plasmopara viticola*. *Vitis,* **47**, 235–240.

Eckardt, N.A. (2004) Host proteins guide *Agrobacterium*-mediated plant transformation. *Plant Cell,* **16**, 2837–2839.

Glawe, D.A. (2008) The powdery mildews: a review of the world's most familiar (yet poorly known) plant pathogens. *Annu. Rev. Phytopathol.* **46**, 27–51.

Goulet, C., Goulet, C., Goulet, M.C. and Michaud, D. (2010) 2-DE proteome maps for the leaf apoplast of *Nicotiana benthamiana*. *Proteomics*, **10**, 2536–2544.

Govindarajulu, M., Epstein, L., Wroblewski, T. and Michelmore, R.W. (2015) Host-induced gene silencing inhibits the biotrophic pathogen causing downy mildew of lettuce. *Plant Biotechnol.* **13**, 875–883.

Hacquard, S. (2014) The genomics of powdery mildew fungi: past achievements, present status and future prospects. *Adv. Bot. Res.* **70**, 109–142.

Higuchi, Y., Nakahama, T., Shoji, J.Y., Arioka, M. and Kitamoto, K. (2006) Visualization of the endocytic pathway in the filamentous fungus *Aspergillus oryzae* using an EGFP-fused plasma membrane protein. *Biochem. Biophys. Res. Commun.* **340**, 784–791.

Jiang, D., Zhu, W., Wang, Y., Sun, C., Zhang, K.Q. and Yang, J. (2013) Molecular tools for functional genomics in filamentous fungi: recent advances and new strategies. *Biotechnol. Adv.* **31**, 1562–1574.

Jovic, M., Sharma, M., Rahajeng, J. and Caplan, S. (2010) The early endosomes: a busy sorting station for the proteins at the crossroads. *Histol. Histopathol.* **25**, 99–112.

Kieleczawa, J. (2006) *DNA Sequencing II. Optimizing Preparation and Cleanup*. Burlington, MA: Jones & Bartlett Learning.

Kulkarni, R.D., Kelkar, H.S. and Dean, R.A. (2003) An eight-cysteine-containing CFEM domain unique to a group of fungal membrane proteins. *Trends Biochem. Sci.* **28**, 118–121.

Lai, E.M. and Kado, C.I. (2000) The T-pilus of *Agrobacterium tumefaciens*. *Trends Microbiol.* **8**, 361–369.

Lawrence, G.J., Dodds, P.N. and Ellis, J.G. (2010) Transformation of the flax rust fungus, *Melampsora lini*: selection via silencing of an avirulence gene. *Plant J.* **61**, 364–369.

Martínez-Cruz, J., Romero, D., Dávila, J.C. and Pérez-García, A. (2014) The *Podosphaera xanthii* haustorium, the fungal Trojan horse of cucurbit–powdery mildew interactions. *Fungal Genet. Biol.* **71**, 21–31.

Martínez-Cruz, J., Romero, D.F., de la Torre, F., Fernández-Ortuño, D., Torés, J.A., de Vicente, A. and Pérez-García, A. (2018) The functional characterization of *Podosphaera xanthii* effector candidate genes reveals novel target functions for fungal pathogenicity. *Mol. Plant–Microbe. Interact.* **31**, 914–931.

Martínez-Cruz, J., Romero, de Vicente, A. and Pérez-García, A. (2017) Transformation of the cucurbit powdery mildew pathogen *Podosphaera xanthii* by *Agrobacterium tumefaciens*. *New Phytol.* **213**, 1961–1973.

Meyers, B., Zaltsman, A., Lacroix, B., Kozlovsky, S.V. and Krichevsky, A. (2010) Nuclear and plastid genetic engineering of plants: comparison of opportunities and challenges. *Biotechnol. Adv.* **28**, 747–756.

Michael, W.L., Robalino, I.V. and Keyhani, N.O. (2009) Uptake of the fluorescent probe FM4-64 by hyphae and haemolymph-derived in vivo hyphal

bodies of the entomopathogenic fungus *Beauveria bassiana*. *Microbiology,* **155**, 3110–3120.

Michielse, C.B., Hooykaas, P.J., van den Hondel, C.A. and Ram, A.F. (2008) *Agrobacterium*-mediated transformation of the filamentous fungus *Aspergillus awamori*. *Nat. Protoc.* **3**, 1671–1678.

Michielse, C.B., van Wijk, R., Reijnen, L., Cornelissen, B.J. and Rep, M. (2009) Insight into the molecular requirements for pathogenicity of *Fusarium oxysporum* f. sp. *lycopersici* through large-scale insertional mutagenesis. *Genome Biol.* **10**, R4.

Nakagawa, T., Kurose, T., Hino, T., Tanaka, K., Kawamukai, M., Niwa, Y., Toyooka, K., Jinbo, T. and Timura, T. (2007) Development of series of gateway binary vectors, pGWBs, for realizing efficient construction of fusion genes for plant transformation. *J. Biosci. Bioeng.* **104**, 34–41.

Nowara, D., Gay, A., Lacomme, C., Shaw, J., Ridout, C., Douchkov, D., Hensel, G., Kumlehn, J. and Schweizer, P. (2010) HIGS: host-induced gene silencing in the obligate biotrophic fungal pathogen *Blumeria graminis*. *Plant Cell,* **22**, 3130–3141.

Panwar, V., McCallum, B. and Bakkeren, G. (2013) Host-induced gene silencing of wheat leaf rust fungus *Puccinia triticina* pathogenicity genes mediated by the *Barley stripe mosaic virus*. *Plant Mol. Biol.* **81**, 595–608.

Park, R.F. and Wellings, C.R. (2012) Somatic hybridization in the Uredinales. *Annu. Rev. Phytopathol.* **50**, 219–239.

Pelczar, P., Kalck, V., Gomez, D. and Hohn, B. (2004) *Agrobacterium* proteins VirD2 and VirE2 mediate precise integration of synthetic T-DNA complexes in mammalian cells. *EMBO Rep.* **5**, 632–637.

Pennington, H.G., Gheorghe, D.M., Damerum, A., Pliego, C., Spanu, P.D., Cramer, R. and Bindschedler, L.V. (2016) Interactions between the powdery mildew effector BEC1054 and barley proteins identify candidate host targets. *J. Proteome Res.* **15**, 826–839.

Pérez-García, A., Romero, D., Fernández-Ortuño, D., López-Ruiz, F., de Vicente, A. and Torés, J.A. (2009) The powdery mildew fungus *Podosphaera fusca* (synonym *Podosphaera xanthii*), a constant threat to cucurbits. *Mol. Plant Pathol.* **10**, 153–160.

Petre, B., Joly, D.L. and Duplessis, S. (2014) Effector proteins of rust fungi. *Front. Plant Sci.* **5**, 416.

Pitzschke, A. (2013) *Agrobacterium* infection and plant defense–transformation success hangs by a thread. *Front. Plant Sci.* **4**, 519.

Pliego, C., Nowara, D., Bonciani, G., Gheorghe, D.M., Xu, R., Surana, P., Whigham, E., Nettleton, D., Bogdanove, A.J., Wise, R.P., Schweizer, P., Bindschedler, L.V. and Spanu, P.D. (2013) Host-induced gene silencing in barley powdery mildew reveals a class of ribonucleases-like effectors. *Mol. Plant–Microbe Interact.* **26**, 633–642.

Ramanujan, R., Calvert, M.E., Selvaraj, P. and Naqvi, N.I. (2013) The late endosomal HOPS complex anchors active G-protein signaling essential for pathogenesis in *Magnaporthe oryzae*. *PloS Pathog.* **9**, e1003527.

Read, N.D. and Kalkman, E.R. (2003) Does endocytosis occur in fungal hyphae? *Fungal Genet Biol.* **39**, 199–203.

Richards, T.A. and Talbot, N.J. (2013) Horizontal gene transfer in osmotrophs: playing with public goods. *Nat. Rev. Microbiol.* **11**, 720–727.

Schillberg, S., Tiburzy, R. and Fischer, R. (2000) Transient transformation of the rust fungus *Puccinia graminis* f.sp. *tritici*. *Mol. Genet. Genomics,* **262**, 911–915.

Schmidt, S.M., Kuhn, H., Micali, C., Liller, C., Kwaaitaal, M. and Panstruga, R. (2014) Interaction of a *Blumeria graminis* f. sp. *hordei* effector candidate with a barley ARF-GAP suggests that host vesicle trafficking is a fungal pathogenicity target. *Mol. Plant Pathol.* **15**, 535–549.

Selin, C., de Kievit, T.R., Belmonte, M.F. and Dilantha Fernando, W.G. (2016) Elucidating the role of effectors in plant–fungal interactions: progress and challenges. *Front. Microbiol.* **7**, 600.

Spanu, P.D, Abbott, J.C, Amselem, J., Burgis, T.A, Soanes, D.M, Stuber, K., Loren van Themaat, E.V, Brown, J.K M, Butcher, S.A, Gurr, S.J, Lebrun, M-H, Ridout, C.J, Schulze-Lefert, P., Talbot, N.J, Ahmadinejad, N., Ametz, C., Barton, G.R, Benjdia, M., Bidzinski, P., Bindschedler, L.V, Both, M., Brewer, M.T, Cadle-Davidson, L., Cadle-Davidson, M.M, Collemare, J., Cramer, R., Frenkel, O., Godfrey, D., Harriman, J., Hoede, C., King, B.C, Klages, S., Kleemann, J., Knoll, D., Koti, P.S, Kreplak, J., Lopez-Ruiz, F.J, Lu, X., Maekawa, T., Mahanil, S., Micali, C., Milgroom, M.G, Montana, G., Noir, S., O'Connell, R.J, Oberhaensli, S., Parlange, F., Pedersen, C., Quesneville, H., Reinhardt, R., Rott, M., Sacristan, S., Schmidt, S.M, Schon, M., Skamnioti, P., Sommer, H., Stephens, A., Takahara, H., Thordal-Christensen, H., Vigouroux, M., Wessling, R., Wicker, T. and Panstruga, R. (2010) Genome expansion and gene loss in powdery mildew fungi reveal tradeoffs in extreme parasitism. *Science,* **330**, 1543–1546.

Stenmark, H. (2009) Rab GTPases as coordinators of vesicle traffic. *Nat. Rev. Mol. Cell. Biol.* **10**, 513–525.

Vela-Corcía, D., Bautista, R., de Vicente, A., Spanu, P.D. and Pérez-García, A. (2016) *De novo* analysis of the epiphytic transcriptome of the cucurbit powdery mildew fungus *Podosphaera xanthii* and identification of candidate secreted effector proteins. *PloS One,* **11**, e0163379.

Vela-Corcía, D., Romero, D., Torés, J.A., de Vicente, A. and Pérez-García, A. (2015) Transient transformation of *Podosphaera xanthii* by electroporation of conidia. *BMC Microbiol.* **15**, 20.

Wang, J.Y. and Li, H.Y. (2008) *Agrobacterium tumefaciens*-mediated genetic transformation of the phytopathogenic fungus *Penicillium digitatum*. *J. Zhejiang Univ. Sci. B,* **9**, 823–828.

Webb, C.A., Szabo, L.J., Bakkeren, G., Garry, C., Staples, R.C., Eversmeyer, M. and Fellers, J.P. (2006) Transient expression and insertional mutagenesis of *Puccinia triticina* using biolistics. *Funct. Integr. Genomics,* **6**, 250–260.

Weβling, R., Schmidt, S.M., Micali, C.O., Knaust, F., Reinhardt, R., Neumann, U., and Ver Loren van Themaat, E. (2012) Transcriptome analysis of enriched *Golovinomyces orontii* haustoria by deep 454 pyrosequencing. *Fungal Genet. Biol.* **49**, 470–482.

Whigham, E., Qi, S., Mistry, D., Surana, P., Xu, R., Fuerst, G., Pliego, C., Bindschedler, L.V., Spanu, P.D., Dickerson, J.A., Innes, R.W., Nettleton, D., Bogdanove, A.J. and Wise, R.P. (2015) Broadly conserved fungal effector BEC1019 suppresses host cell death and enhances pathogen virulence in powdery mildew of barley (*Hordeum vulgare* L.). *Mol. Plant–Microbe Interact.* **28**, 969–983.

SUPPORTING INFORMATION

Additional Supporting Information may be found in the online version of this article at the publisher's website:

Table S1 Transfer DNA (T-DNA) border flanking sequences of four selected *Podosphaera xanthii* transformants obtained after agro-infiltration with the plasmids pPK2-hphgfp (t3-t4) and pPK2Tgfp (t5-t6).

Table S2 BLAST analysis of thermal asymmetric interlaced-polymerase chain reaction (TAIL-PCR) products obtained from the flanking sequences of the T-DNA regions of four *Podosphaera xanthii* transformants obtained after agro-infiltration with the plasmids pPK2-hphgfp (t3-t4) and pPK2Tgfp (t5-t6).

Table S3 Oligonucleotides used in this study.

Fig. S1 Schematic representation of the transfer DNA (T-DNA) in the vectors used in our study.

Fig. S2 Analysis of the persistence of *Agrobacterium tumefaciens* cells on the surface of melon cotyledons after agro-infiltration and cefotaxime treatment.

Fig. S3 Agro-infiltration of transfer DNA (T-DNA) constructs results in the acquisition of phenotypes by *Podosphaera xanthii*.

Fig. S4 Bright field and epifluorescence micrographs of agro-infiltrated melon cotyledons.

Fig. S5 Epifluorescence microscopy analysis of cotyledons transformed with transfer DNA (T-DNA) of pPK2-hphgfp and inoculated with *Podosphaera xanthii*.

Fig. S6 Molecular analysis of *Podosphaera xanthii* transformants obtained after agro-infiltration.

Fig. S7 Thermal asymmetric interlaced-polymerase chain reaction (TAIL-PCR) analysis of flanking sequences of transfer DNA (T-DNA) regions of four random transformants.

Fig. S8 Alignment of the cysteine-rich fungal extracellular membrane (CFEM) domain-containing proteins EC2 from various powdery mildew fungi.

Fig. S9 Epifluorescence microscopy analysis of a *Podosphaera xanthii* colony transformed with the transfer DNA (T-DNA) of pPK2-PxEC2gfp.

Fig. S10 Bright field and epifluorescence micrographs of *Podosphaera xanthii* transformed colonies.

Fig. S11 Epifluorescence microscopy analysis of a *Podosphaera xanthii* colony growing on a leaf zone agro-infiltrated with pGWB6-egfpVirD2.

Fig. S12 Subcellular localization of the *Agrobacterium* protein VirD2 in a haustorium of *Podosphaera xanthii*.

Fig. S13 Subcellular localization of *Agrobacterium* protein VirD2 and the endocytosis vesicle-associated fungal protein Rab5 in *Podosphaera xanthii* transformants.

Fig. S14 Schematic representation of the model of transfer DNA (T-DNA) integration into the *Podosphaera xanthii* genome after agro-infiltration and pathogen inoculation.